

This article appeared in a journal published by Elsevier. The attached copy is furnished to the author for internal non-commercial research and education use, including for instruction at the authors institution and sharing with colleagues.

Other uses, including reproduction and distribution, or selling or licensing copies, or posting to personal, institutional or third party websites are prohibited.

In most cases authors are permitted to post their version of the article (e.g. in Word or Tex form) to their personal website or institutional repository. Authors requiring further information regarding Elsevier's archiving and manuscript policies are encouraged to visit:

<http://www.elsevier.com/copyright>



Contents lists available at ScienceDirect

Nuclear Instruments and Methods in Physics Research A

journal homepage: www.elsevier.com/locate/nima

Advanced X-ray radiography and tomography in several engineering applications

Daniel Vavrik^{a,b,*}, J. Dammer^a, J. Jakubek^a, I. Jeon^c, O. Jirousek^b, M. Kroupa^a, P. Zlamal^b^a Institute of Experimental and Applied Physics of the Czech Technical University in Prague, Horska 3a/22, 128 00, Prague 2, Czech Republic^b Institute of Theoretical and Applied Mechanics of the Czech Academy of Sciences, Prosecka 76, 190 00, Prague 9, Czech Republic^c School of Mechanical Systems Engineering of the Chonnam National University, 300 Yongbong-dong, Buk-gu, Gwangju, 500-757, Republic of Korea

ARTICLE INFO

Available online 17 June 2010

Keywords:

Beam hardening correction
Flat fiel correction
Digital radiography

ABSTRACT

New developments in the fields of X-ray detectors, X-ray micro/nano sources and data processing bring new possibilities for engineering practice in many applications. Nowadays it is possible to observe an object, which was difficult to image before due to limitations such as low contrast, low dynamic range, low attenuation and/or small structural dimensions. A number of compelling problems in different applications are summarized. Digital radiograms in this work are acquired using micro- and nano-focus X-ray tubes together with semiconductor digital pixelated detectors. A beam hardening correction was done for relevant radiograms and an iterative OSEM (ordered subsets) method was applied for CT reconstructions.

© 2010 Elsevier B.V. All rights reserved.

1. Introduction

Progress in engineering for radiography has been significant in recent years. X-ray sources, the first microfocus (several μm spot size) tubes, became available at the beginning of this decade and nanofocus tubes ($\sim 1 \mu\text{m}$ spot size) came on the market few years later. These tubes allow one to observe structures with size several micrometers, respectively, several hundreds of nanometers (actual resolution depends on X-ray source spot size together with the geometrical projection magnification). Nowadays open tubes moreover allow one to change the target, enabling different X-ray spectra to be chosen for particular tasks.

Non-direct and direct X-ray converting semiconductor detectors are an equally important part of digital radiography with a similarly recent history. Semiconductor detectors exhibit high sensitivity and high dynamic range. Some semiconductor detectors even have spectroscopic properties, which can be important for material resolving radiography.

Digital radiography has brought routine accessibility of advanced methods such as modular computed tomography, low energy, material resolving (spectroscopic) and high dynamic range radiography. Some examples of these techniques developed in our laboratory are presented below.

* Corresponding author at: Institute of Experimental and Applied Physics of the Czech Technical University in Prague, Horska 3a/22, 128 00, Prague 2, Czech Republic. Tel.: +420 224 359 181; fax: +420 224 359 392.

E-mail address: daniel.vavrik@utef.cvut.cz (D. Vavrik).

2. Advanced digital radiography examples

2.1. Modular computed tomography system

Medical and industrial tomography systems usually have a stable detector type and limited variability of the projection geometry. These restrictions allow system only optimization for a given object; other specimen types are hard to inspect with satisfactory quality. Our tabletop laboratory system [1] allows one to exchange the detector after the projection distance and the manipulation stage type. This modularity brings the possibility of inspecting a wide range of different objects.

For high resolution, low energy and spectroscopic radiography the Medipix type detector [2] is utilized. A flat panel detector Hamamatsu (C7942CA with CsITl scintillator) is mainly employed for large objects and for materials with higher attenuation. A Fein focus tube with an exchangeable head and target is used as micro/nanofocus divergent beam source ($1\text{--}5 \mu\text{m}$ spot size depending on regime applied). A CT system is used for simple transmission radiography as well.

Beam hardening effect is *standardly* corrected using the signal to equivalent thickness (SET) calibration method in our laboratory [3,4]. The numerical method of ordered subsets expectation maximization—OSEM [3]—is implemented for computed tomography reconstruction software in our laboratory.

The tomographic reconstruction of a coneiform tablet is presented in Fig. 1 as first example. Reading coneiforms requires manipulation and observation from all angles when an expert tries to decipher coneiforms. For this reason, a virtual

model given by a CT is advantageous to preserve the tablets intact. A flat panel was used as imager. Cuneiforms are easily recognizable even though they appear relatively shallow in comparison with tablet thickness. The OSEM method gives good results although outside object boundaries are not usually well defined when only standard filtered back projection is applied.

As a routine task in cultural heritage, historical wooden structures have to be evaluated. A CT reconstruction of a wood sample damaged by woodworm and rot is depicted in Fig. 2. Winter and summer wood as well as knot structures are easily recognizable. The nog cross-section is $50 \times 50 \text{ mm}^2$ and is obviously radiographically almost transparent. Aluminum cover of the flat panel was removed to utilize the lower energy photons for which better contrast is obtained. The flat panel used is sensitive down to 10 keV approximately.

2.2. High dynamic range radiography

An important advantage of the Medipix device is its practically unlimited dynamic range, thanks to zero dark signal. The noise in the image is given just by the statistical nature of the number of photons hitting the pixel. Consequently the signal to noise ratio can be improved by a higher number of detected photons.



Fig. 1. Ceramic cuneiform tablet (80 mm in height and 15 mm in thickness).

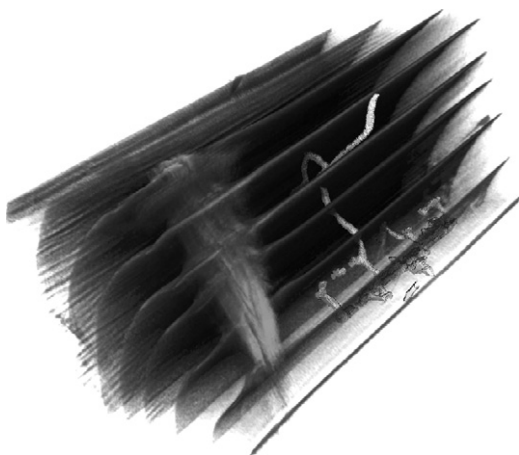


Fig. 2. A wood bar, $100 \times 50 \times 50 \text{ mm}^3$.

This feature allows reaching almost arbitrary contrast in measured images just by prolongation of exposure time.

As a very important task in the aerospace industry, a high contrast image of a fatigue crack is demonstrated in Fig. 3. The fatigue crack developed in the glass-epoxy layer and was shielded by a rivet head and Al-alloy layer. Such shielded cracks can be otherwise made visible only when the related components are dismantled.

This internal crack and inner glass fiber structure are radiographically visible, thanks to the high 15 bit dynamic range of this radiogram (it is a real number of detected photons in one pixel). The crack resolved occupies just 3% of this dynamic range. A sequence of six hundred snapshots with 1-s exposition was measured (tungsten tube at 70 kV).

2.3. Low energy radiography

Low energy radiography (below 10 keV) is ideal for very thin and very low absorption objects. The Medipix MXR detector [5] used has sensitivity down to 4 keV with negligible noise.

Two related examples are depicted in Fig. 4—a micro CT of a sand-clay and cellulose samples. These materials, which are used for desalting, require for this purpose that their porosity be evaluated. Pores in the sand-clay sample (left) are relatively small, so a CT has to have high contrast to distinguish the pore boundaries. Although the cellulose sample (right) is essentially transparent for X-rays, it is possible to recognize its inner structure.

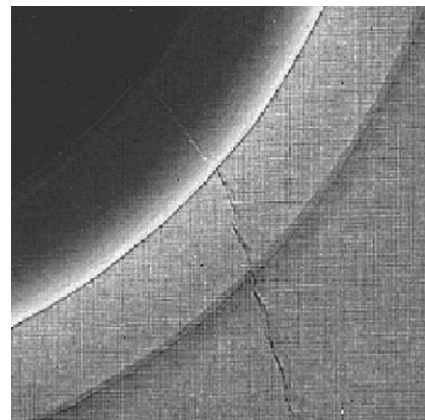


Fig. 3. Radiography of a crack inside a laminate layer. Dimension of this image is $1.5 \times 1.5 \text{ mm}^2$.

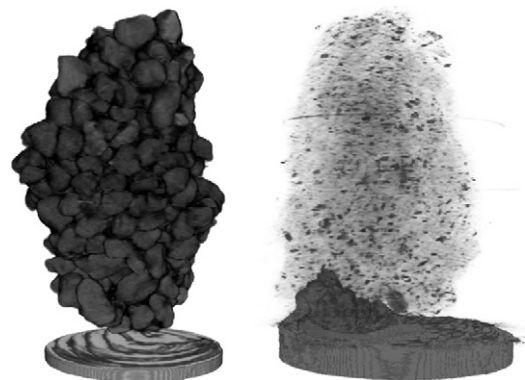


Fig. 4. Reconstruction of the sand-clay (left) and cellulose (right) samples. These are approximately 5 mm high.

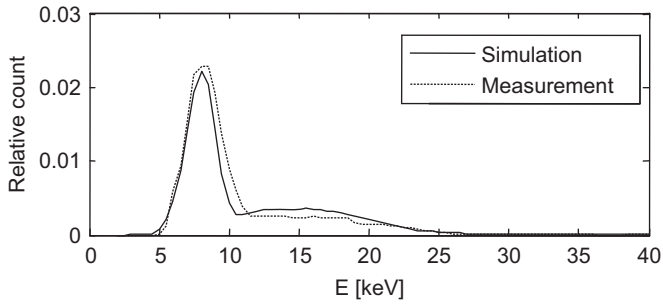


Fig. 5. Spectra behind Cu sheet measured and simulated for one individual detector pixel.

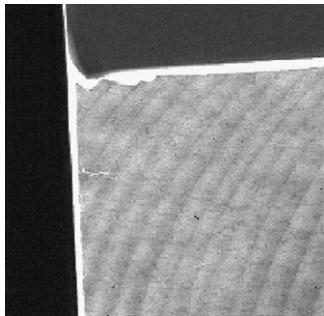


Fig. 6. Radiogram of a specimen with copper strip (left) aluminum (top) and Al alloy (bottom).

2.4. Material resolving radiography

Since the TimePix pixel single photon counting detector [6] from Medipix family is energy sensitive, we can use it for measuring the energy spectra of the X-ray beam transmitted through the inspected sample. The event-by-event measurement has to be performed with a low X-ray photon flux to avoid overlapping of individual events in individual pixels. The resultant transmission spectrum has characteristic shape depending specimen thickness and material composition. Consequently specimen thickness profile and its composition can be separated by fitting of measured spectra.

A demonstration sample was prepared from three pieces of thin sheets manufactured from copper, aluminum and aluminum alloy [7]. The photoelectric absorption was assumed for spectra simulation. Spectra measured and simulated for X-rays behind copper are given in Fig. 5. The relative amount of Cu, Al, Fe, Si and total thickness in related pixel were varied to reach such spectra. Fig. 6 shows the original radiogram. The distribution of copper calculated from the spectra is depicted in Fig. 7 and aluminum distribution is imaged in Fig. 8. The thickness profile is depicted in Fig. 9.

2.5. High resolution radiography of a steel sample

The inner structure of a 3 mm thick steel sample is not easy to recognize, thanks to intensive photon scattering. It was necessary to prefilter the X-ray beam using a 0.7 mm thick brass sheet to suppress this effect. The beam is significantly hardened in this way; effective energy was approximately 50 keV. The Medipix detector with 300 μm silicon sensor is not sensitive enough for such energy and 150 μm long crack is practically undetectable while it is visible using a flat panel (see Fig. 5). However the influence of dark current was significant for flat panel image quality (pronounced as vertical structure in this image) (Fig. 10).

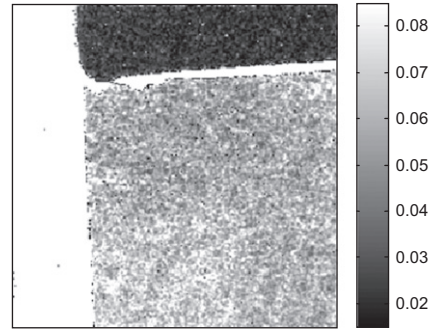


Fig. 7. Cu relative volume fraction in whole object. The irregular Cu distribution in the Al alloy is visible.

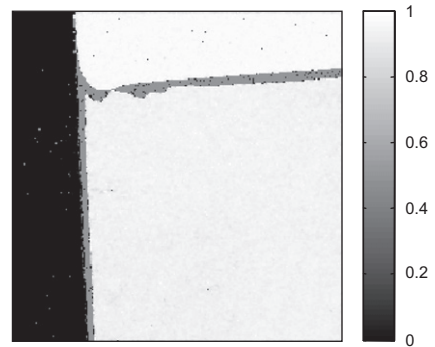


Fig. 8. Al relative volume fraction.

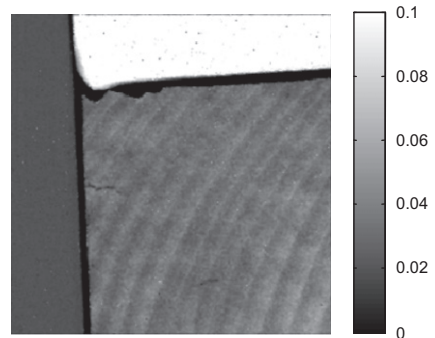


Fig. 9. The specimen thickness profile in mm scale.

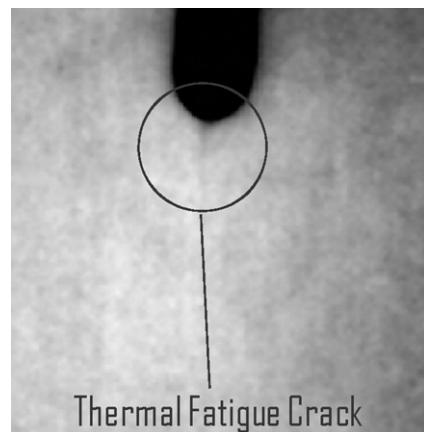


Fig. 10. The specimen thickness profile in mm scale. Width of this image is ~4 mm.

3. Conclusions

It has been proven that modular computed tomography system alternatively equipped by the two digital X-ray imagers allows inspecting a wide range of the object with various dimensions and material properties with excellent quality of the radiograms obtained.

Choosing of specific X-ray imaging system depends on the object type inspected and on the required results:

- The Medipix detector has great performance in the very low energy range and for the objects where high contrast of the radiograms is required.
- Medipix/Timepix detector is a powerful tool for material analysis with respect to spectroscopic properties of this device.
- Flat panel is advantageous for larger objects and for higher X-ray energies.

Radiograms and CT reconstructions quality are significantly enhanced in our work, thanks to appropriate data processing, namely beam hardening correction (using the signal to equivalent thickness method) and advanced iterative technique for CT

reconstruction (method of ordered subsets expectation maximization—OSEM).

Acknowledgements

This work was carried out in frame of the CERN Medipix Collaboration and has been supported by the Project LC06041, AV0Z20710524 and 6840770040 of the Ministry of Education, Youth and Sports of the Czech Republic. This work has been supported in part by Research Grant no. 103/09/2101 of the Grant Agency of the Czech Republic and by the Ministry of Education.

References

- [1] J. Jakůbek, D. Vavřík, T. Holý, M. Jakůbek, Z. Vykydal, Nucl. Instr. and Meth. A 563 (2006) 278.
- [2] Medipix collaboration home page, <<http://medipix.web.cern.ch/MEDIPIX/S>>.
- [3] J. Jakůbek, Nucl. Instr. and Meth. A 576 (2007) 223.
- [4] D. Vavřík, Nucl. Instr. and Meth. A 607 (2009) 212.
- [5] X. Llopart, M. Campbell, R. Dinapoli, D. San Segundo, E. Pernigotti, IEEE Trans. Nucl. Sci., 49:2279–2283, 2001.
- [6] X. Llopart, R. Ballabriga, M. Campbell, L. Tlustos, W. Wong, Nucl. Instr. and Meth. in Phys. Res. A 581 (2007) 485.
- [7] D. Vavřík, J. Jakůbek, Material analysis using characteristic transmission spectra, in: Proceedings of the Conference Record of the 2008 IEEE NSS/MIC/RTSD, 2008.